



	Experiment title: Time resolved study of microstructure and interface evolution during simulated steel welding.	Experiment number: MA1358
Beamline: ID15A	Date of experiment: from: 30/11/2011 to: 05/12/2011	Date of report: 04/03/2013
Shifts: 18	Local contact(s): Marco Di Michiel	<i>Received at ESRF:</i>
Names and affiliations of applicants (* indicates experimentalists): Ragnvald Mathiesen* :Dept. of Physics, NTNU, N-7491 Trondheim, Norway Wajira Mirihanage* :Dept. of Physics, NTNU, N-7491 Trondheim, Norway Lars Arnberg :Dept. of Materials Science and Engineering, NTNU, N-7491 Trondheim, Norway.		

Report:

Simulated welding of Austenitic steel (Cr-17.3%, Ni-11.1%, Mo-2.1% C<0.1%) has been studied in situ via ultrafast polychromatic XRD. The experimental weld simulation rig consisted of seven 1kW halogen lamps assembled with elliptical reflectors to a common focus on the sample surface creating ~ 6 mm diameter weld pool within ~2 seconds. The sample was placed in a boron-nitride support in direct thermal contact with a secondary resistive heater, with intended purpose primarily to allow for regulating the cooling rate during re-solidification of the pool. The weld pool was positioned in the incident ID15A polychromatic X-ray beam (main photon energy range 50-150 keV), in a near-horizontal position at an inclination angle of 2°, slitted to a 1.0 x 0.1 mm² cross-section roughly symmetric about the centre of the weld pool surface. 2D XRD data was collected during melting and subsequent solidification of the pool, spanning an angles $2\theta < 16^\circ$ in the upper left hemispherical forward scattering quadrant, at a 1 kHz frame rate. The upper right quadrant was reserved to another set of measurement comprising two additional detectors; one used primarily for low-resolution diffraction spot selection in order to align the second one functioning as a high-resolution (HR) detector focused at the selected spot. The intention with this part of the experiment was to allow for collection of time-resolved “white-beam reflection topograms” to reveal explicit details on the morphological evolution of individual grains. The camera frame rate used for the topography experiments was 0.5 kHz. Totally 26, simulated melting-welding cycles were conducted with the Austenitic steel, and additional 20 sequences were collected with AA 5XXX weldable Al-alloys for comparison primarily, all in all comprising almost 2TB of raw data.

The sequences collected had a typical duration 3–5 s for the complete melting-freezing cycle, with the re-solidification period started roughly at the middle of the intervals by switching off the halogen heaters as soon as complete melting within the volume irradiated by the incident beam was verified. Until now, no efforts have been made to analyse the melting process, in this report and in forthcoming paper submissions focus will be devoted to the solidification. Still, analysis of the melting stage is also scientifically interesting, and may commence at a later stage.

Prominent to all sequences was a remarkable angular motion of individual diffraction spots, in particular in the early stages of solidification. The observation is ascribed to grain rotation and bending due to a relatively massive convection present in the weld-pool melt. In fact, the presence of convection was evident also in the post-welded samples which typically showed pitting in the centre of the weld, and also that advective currents had moved melt outside the initial pool leaving a continuous protruded ring of solidified material outside its edges. Due to the fierce angular dynamics, the HR magnified topography measurements turned out virtually impossible. The HR-detector operates with a small aperture thin transparent scintillator optically magnified onto the camera, thus fast-moving diffraction spots are blurred and move across the entire field of view in just a few frames. Accordingly, it was readily realised that the ability to capture useful topography images from the experiments were beyond the current technical capabilities, despite utilising the highest X-ray photon flux and the fastest detectors available, and thus, our efforts in the post experimental processing have been concentrated exclusively on the vast amounts of solidification data collected via in-situ ultra-fast XRD. If the angular motion had been limited to thermal contraction only, where frame-to-frame motion is modest and the angular trajectory is predictable, it would have sufficed to move the camera at low velocities along the trajectory to keep the pre-selected spot in camera. However, the angular velocities we observed were up to 3 orders of magnitude above those associated with lattice contraction at cooling rates ~ 200 K/s, and with non-predictable trajectories. In fact, thermal contraction effects become clearly visible and easy to distinguish as soon as the weld-pool solid fraction has reached 0.4, and the solid network becomes fully coherent and the impact of flow is reduced.

The information extracted from processing of the XRD data reveals individual time-resolved dendrite growth rates and overall solidification rates in the weld pools during their freezing. In addition the data has been processed in terms of the angular rotations in order to extract information also on melt convection and advection via relatively simplistic model-assumptions concerning liquid-solid momentum transfer in the early stages of growth, when the effects are most prominent. In the processing, raw XRD data have been converted into quantitative data on individual grain volume evolution and motion, based on integrated intensities, morphological rendering and motion-tracking of individual diffraction spots via a suit of custom built routines, which also took care of all required scalings and corrections.

A selection of individual grain growth curves, together with the overall solid fraction curve (f_s) is illustrated in Fig.1. Extracting the slopes of such data, reveal growth velocities up to 3 mm/s (as is the case for grain 4 in the figure). Most of the growth data selected and analysed correspond to columnar grains that grow with primary tip directions at angles $< 15^\circ$ with respect to the incident beam direction. Since the vertical size of the beam is rather small, this would mainly be grains that grow in the surface-near region toward the weld centre. This was a chosen geometry for this experiment, but also other alignments should be possible to realise. For the cases illustrated in Fig. 1, grains 1-3 and grain 6 falls within this category, whereas grain 4 grows in a direction with a larger component along the surface normal, and therefore eventually grows outside the X-ray illuminated region. Grain 5 is a late arriver which grows in from the side in a direction which makes a high angle with the incident beam.

In the early stages of solidification grain motion was particularly rapid, and by support from post-welding SEM and metallographic investigations, these rapid motions have been confirmed to relate to rotation of free equiaxed grains, probably formed by fragmentation of early stage columnar dendrites at the initial melt-solid interface. By analysis, grain rotations can be converted to metric velocities, and the fastest motions detected for free crystals are up to 10 mm/s. Another grain rotation regime occurring at early and intermediate stages could be ascribed to bending/torque of columnar grains. These rotations were associated with lower velocities than the free grains, at maximum 2-3 mm/s at very early stages, as illustrated with the case shown in Fig.2. By successful indexing of a few reflection pairs belonging to the same columnar grain, in addition to indexing growth directions ([100]-type strongly preferred for the present alloy) of the grains that remain bathed in the incident beam and therefore must grow predominantly at a low angle with respect to it, allowed for some of the rotations to be analysed in more detail. For these cases, grain bending both at its attaching root and along the primary columnar trunk was found to be dominant, and there was barely any sign of torque. This seems consistent with liquid-solid momentum transfer being caused by shear flow at the columnar growth fronts, and possibly also some contribution from mechanical impingement between columnar stalks with non-parallel growth directions.

To our knowledge this is the first experimental data ever to report on individual grain growth and overall solid fraction evolution in real weld pools. Furthermore such grain rotations, motions or liquid-solid momentum transfer is novel in the case of welding or similar rapid solidification processing, and is, to our knowledge, not incorporated in any simulation models, although its presence should be well-recognized as such situations are commonly handled for solidification fronts in many models for conventional casting. In processes where high cooling rates apply advection and convection should be expected to be prominent mechanisms for heat and mass transport, and the reason for not incorporating such may only be justified by a complete lack of relevant experimental data.

The derived columnar dendrite growth rates and rotation velocities are of the same order of magnitude, which serves to underline the role of liquid flow as a controlling mechanism for the dendrite growth, at least in the early and intermediate stages of welding. The experimental results serves to stress that melt flow and liquid to solid momentum transfer must be properly addressed in future theory and simulation models for weld solidification, rather than relying on direct extrapolation of conditions and exchange terms used for ordinary transient solidification processes.

The first results on rapid solidification dynamics is currently in preparation for a publication in a high impact journal. An international conference publication and a second journal publication with further data analysis is also on its way. The MA1358 experimental results are also being used to guide and validate multi-scale weld solidification models developing in the EC-FP7 project MintWeld. Finally, the experimental method devised herein should be possible to extend to welding in a more general manner, i.e. with other high melting temperature steels and Ni superalloys, in situ and in operando with real welding tools.

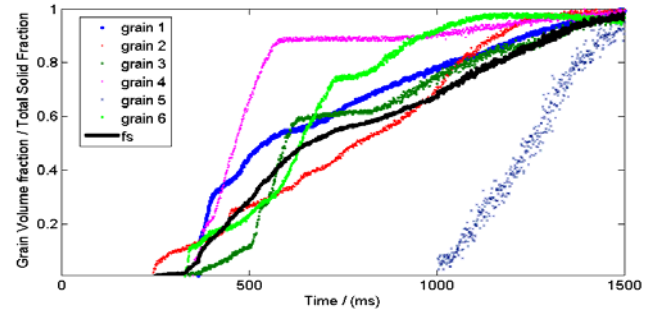


Figure 1. Time evolution of individual dendrite volumes and overall solid fraction

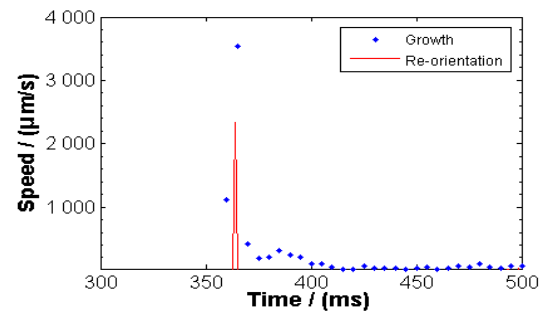


Figure 2. Growth and re-orientation rate evolution of a single dendrite.